
Figures and figure supplements

A model symbiosis reveals a role for sheathed-flagellum rotation in the release of immunogenic lipopolysaccharide

Caitlin A Brennan, et al.

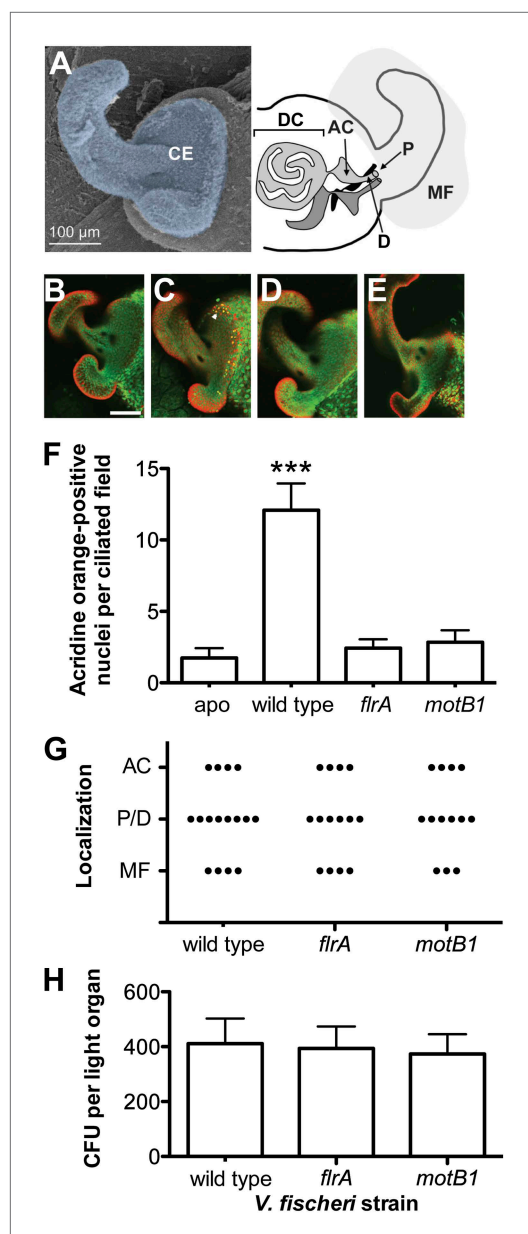


Figure 1. Motility mutants of *V. fischeri* do not induce early-stage apoptosis. **(A)** Morphology of the juvenile light organ, highlighting the external ciliated epithelium (CE; false-colored blue) in a scanning electron micrograph (left), and the internal features with which the bacteria interact during initiation of symbiotic colonization in a schematic diagram (right). DC, deep crypts; AC, antechamber; D, duct; P, pore; and MF, mucus field. **(B–E)** Representative laser-scanning confocal microscopy (LSCM) images of acridine orange (AO)-stained juvenile light organs, after exposure to either: no *V. fischeri* (**B**, apo); wild type (**C**); *flrA* (**D**); or *motB1* (**E**), as described in the 'Materials and methods'. White arrowhead in (**C**) indicates one of the numerous AO-positive nuclei (yellow). Scale bar in (**B**) represents 100 μm for all the images. **(F)** Counts of AO-positive nuclei per ciliated field for different *V. fischeri* strains. *** indicates statistical significance (p < 0.001). **(G)** Localization of bacteria in the juvenile light organ for wild type, *flrA*, and *motB1* strains. Localization is indicated by dots. **(H)** Counts of CFU per light organ for different *V. fischeri* strains.

Figure 1. Continued

nuclei in the light-organ ciliated epithelium of squid exposed to either the indicated *V. fischeri* strains, or no *V. fischeri* (apo). (***), $p < 0.001$ by Kruskal–Wallis Analysis of Variance (ANOVA), followed by Dunn’s Multiple Comparison test. The absence of apoptosis in the aposymbiotic squid confirms that the experimental addition of peptidoglycan (PGN) (‘Materials and methods’) is insufficient to induce AO staining. (G) Bacterial localization under conditions used for measurement of early-stage apoptosis (panel F). Localization was determined by examining squid exposed to the indicated strains, genetically labeled to express GFP, using LSCM. Each point represents the bacterial localization in a single light-organ lobe. (H) Level of colonization (colony-forming units, CFU) under conditions used for measurement of early-stage apoptosis (panel F). Light organs were dissected from anesthetized and pithed squid, and then homogenized and plated to determine symbiont number.

DOI: [10.7554/eLife.01579.003](https://doi.org/10.7554/eLife.01579.003)

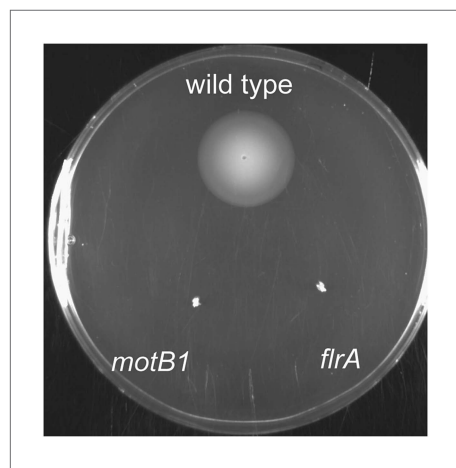


Figure 1—figure supplement 1. Soft-agar motility of wild-type, *flrA* and *motB1* strains.

DOI: [10.7554/eLife.01579.004](https://doi.org/10.7554/eLife.01579.004)

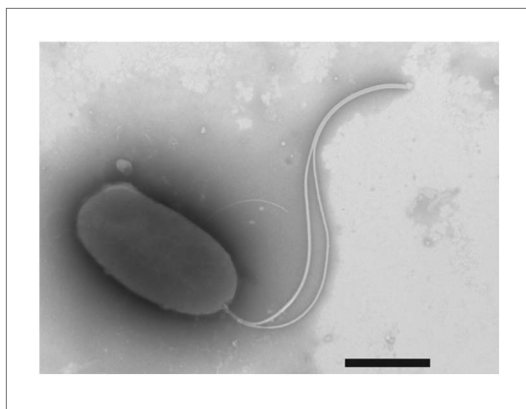


Figure 1—figure supplement 2. Negative-stain transmission electron micrograph of a representative flagellated *motB1* cell.

DOI: [10.7554/eLife.01579.005](https://doi.org/10.7554/eLife.01579.005)

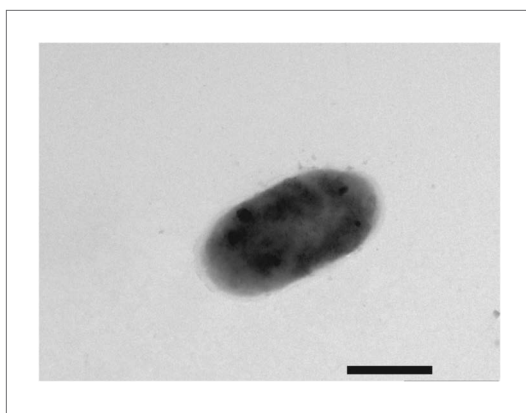


Figure 1—figure supplement 3. Negative-stain transmission electron micrograph of a representative aflagellate *flrA* cell.

DOI: [10.7554/eLife.01579.006](https://doi.org/10.7554/eLife.01579.006)

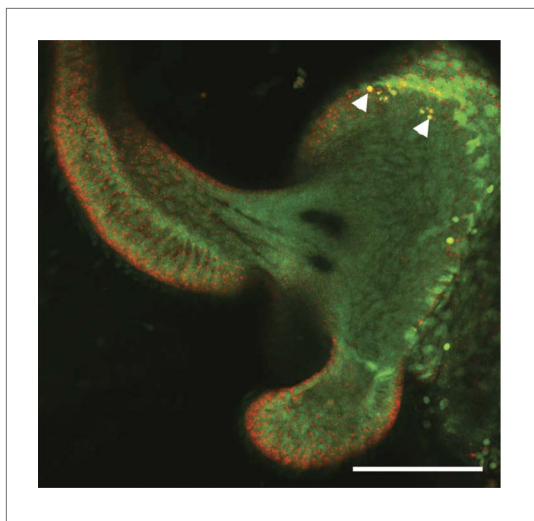


Figure 1—figure supplement 4. Representative LSCM image of an AO-stained light-organ lobe isolated from a squid treated with exogenous *V. fischeri* lipid A.

DOI: [10.7554/eLife.01579.007](https://doi.org/10.7554/eLife.01579.007)

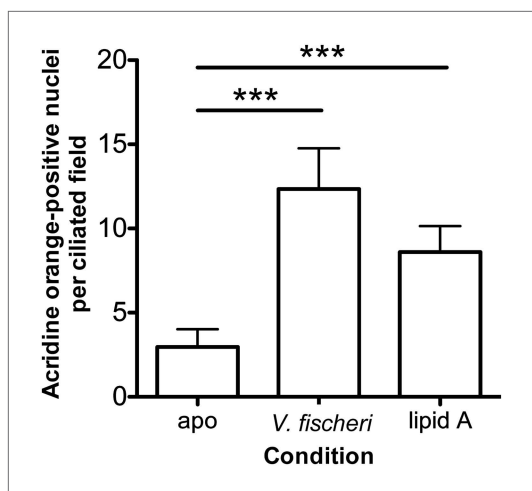


Figure 1—figure supplement 5. Induction of early-stage apoptosis in response to exogenous lipid A.

DOI: [10.7554/eLife.01579.008](https://doi.org/10.7554/eLife.01579.008)

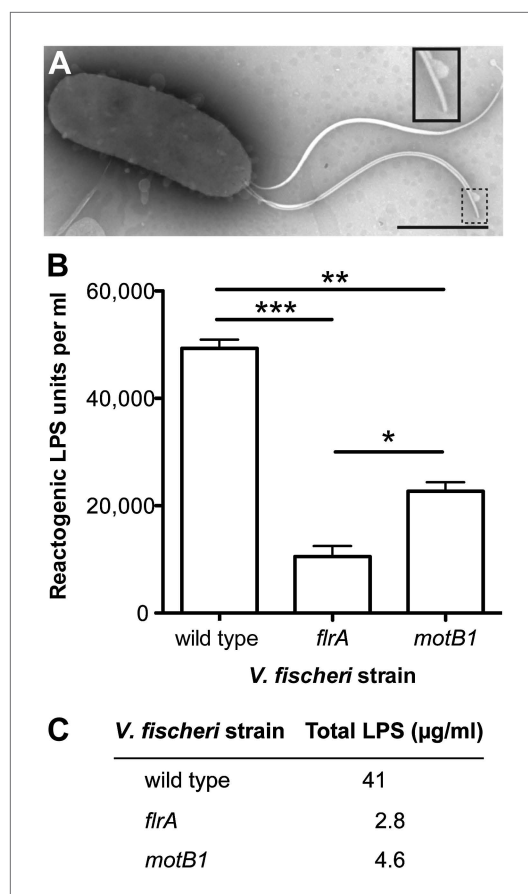


Figure 2. Motility mutants of *V. fischeri* release less LPS into culture supernatants. **(A)** Negative-stain TEM of a wild-type *V. fischeri* cell. Dashed box, shown larger within the solid box, highlights the distal tip of two flagella, one of which displays dissociation of the sheath from the filament in the form of a membrane vesicle-like structure. Scale bar indicates 1 μm . **(B)** Reactogenic LPS in cell-free supernatants of *V. fischeri* mid-log ($\text{OD}_{600} \approx 0.5$) cultures grown in seawater tryptone (SWT) medium at 28°C was measured by LAL assay. (*), $p < 0.05$; (**), $p < 0.01$; and (***), $p < 0.001$, as analyzed by one-way repeated measures ANOVA, with a posthoc Bonferroni correction. **(C)** Total LPS levels in cell-free supernatants from mid-log ($\text{OD}_{600} \approx 0.5$) cultures grown in SWT at 28°C for indicated strains were determined by quantitative SDS-PAGE analysis (detailed in **Figure 2—figure supplement 1**).

DOI: [10.7554/eLife.01579.009](https://doi.org/10.7554/eLife.01579.009)

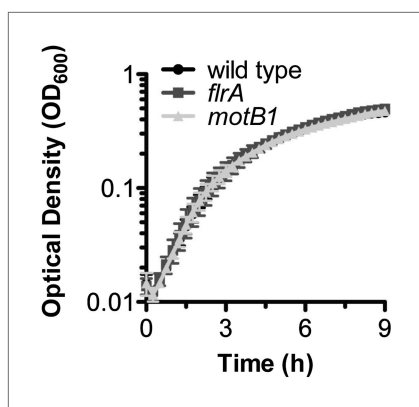


Figure 2—figure supplement 1. Growth of *V. fischeri* wild-type, *motB1* and *flrA* strains.

DOI: [10.7554/eLife.01579.010](https://doi.org/10.7554/eLife.01579.010)

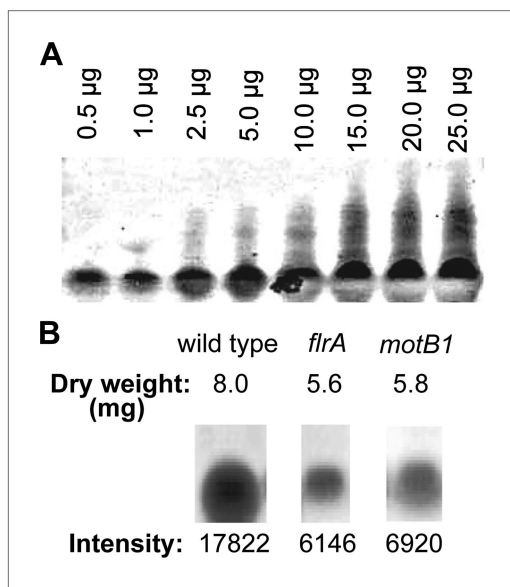


Figure 2—figure supplement 2. Quantification of total LPS in cell-free supernatants by SDS-PAGE analysis.

DOI: [10.7554/eLife.01579.011](https://doi.org/10.7554/eLife.01579.011)

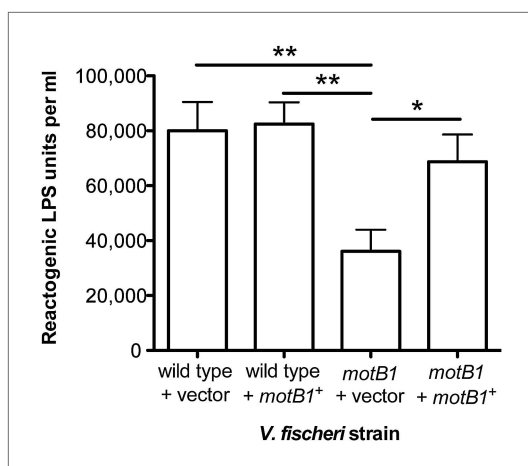


Figure 3. Genetic complementation restores supernatant LPS levels to the *motB1* mutant strain. Levels of reactogenic LPS in mid-log culture supernatants ($OD_{600} \approx 0.5$) of indicated strains, as measured using the LAL assay. (*), $p < 0.05$, and (**), $p < 0.01$, as analyzed by one-way repeated measures ANOVA with a posthoc Bonferroni correction. DOI: [10.7554/eLife.01579.012](https://doi.org/10.7554/eLife.01579.012)

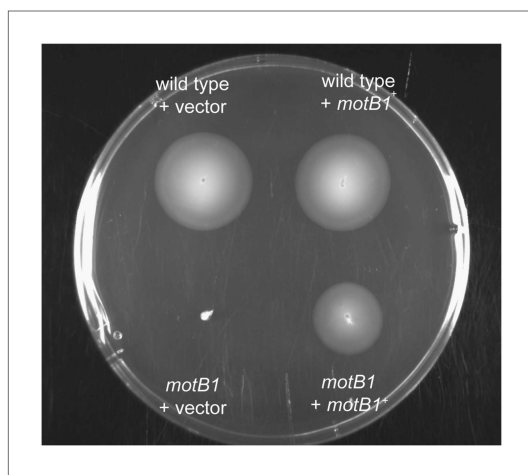


Figure 3—figure supplement 1. Soft-agar motility of genetically complemented *motB1* strains. DOI: [10.7554/eLife.01579.013](https://doi.org/10.7554/eLife.01579.013)

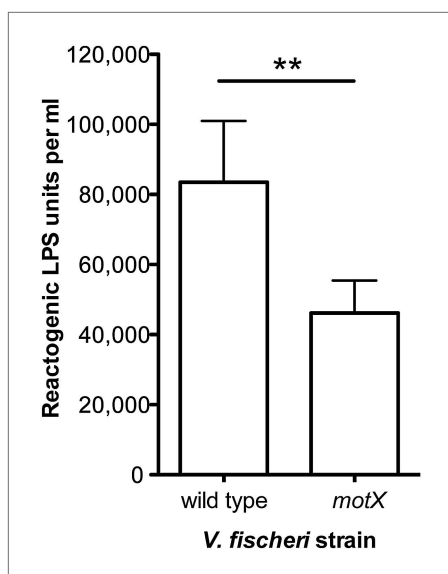


Figure 4. Disruption of *motX* in *V. fischeri* reduces supernatant LPS levels. Levels of reactogenic LPS, as measured using the LAL assay, in cell-free supernatants of mid-log cultures ($OD_{600} \approx 0.5$) of *V. fischeri* wild-type and *motX* strains. (**), $p < 0.01$ as determined by paired Student's *t* test.

DOI: [10.7554/eLife.01579.014](https://doi.org/10.7554/eLife.01579.014)

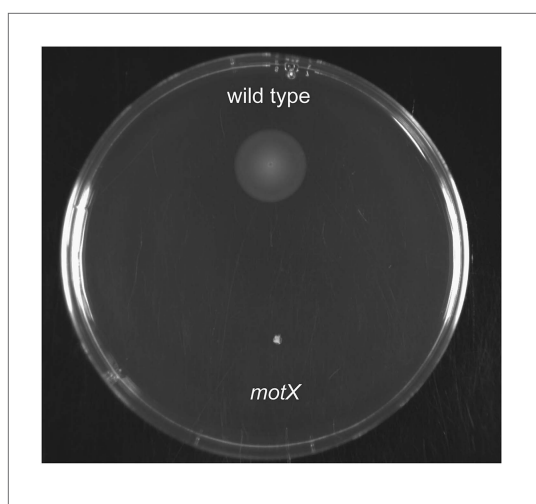


Figure 4—figure supplement 1. Soft-agar motility of *V. fischeri motX* mutant.

DOI: [10.7554/eLife.01579.015](https://doi.org/10.7554/eLife.01579.015)

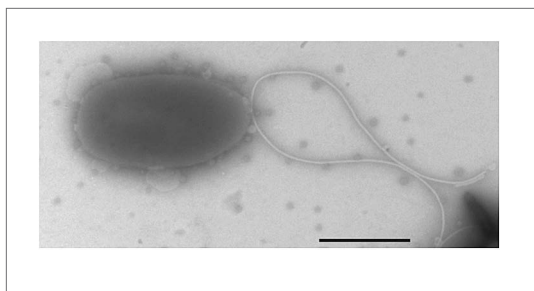


Figure 4—figure supplement 2. Negative-stain transmission electron micrograph of a representative *motX* cell.

DOI: [10.7554/eLife.01579.016](https://doi.org/10.7554/eLife.01579.016)

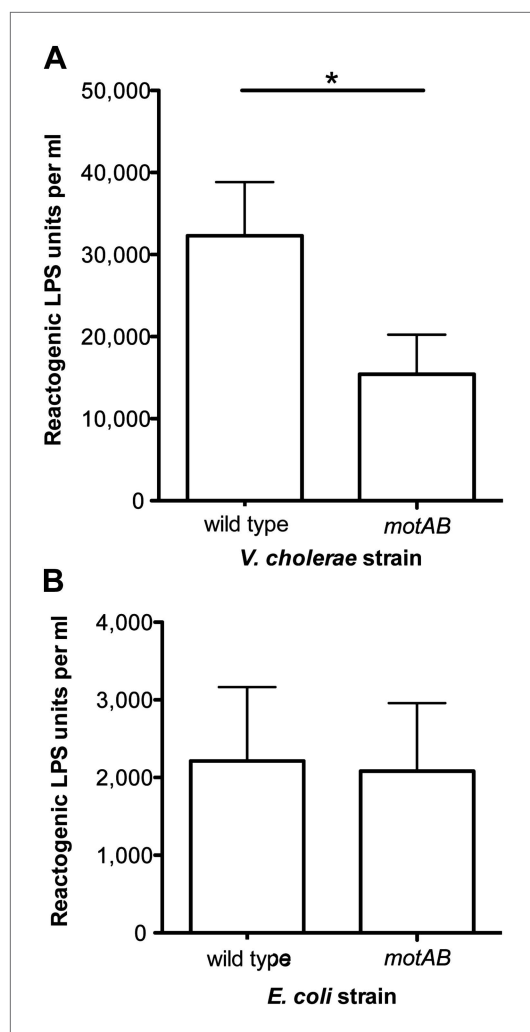


Figure 5. Loss of flagellar rotation reduces LPS release by sheathed *V. cholerae*, but not unsheathed *E. coli*. **(A)** Reactogenic LPS released into mid-log ($OD_{600} \approx 0.5$) culture supernatants by wild-type *V. cholerae* O395N1 and its *motAB* (i.e., *pomAB*) derivative, grown in SWT at 37°C, was measured by the LAL assay. (*), $p < 0.05$ by paired Student's *t* test. **(B)** Reactogenic LPS in mid-log ($OD_{600} \approx 0.5$) culture supernatants of wild-type *E. coli* and its *motAB* derivative grown in tryptone medium at 30°C, as measured using the LAL assay.

DOI: [10.7554/eLife.01579.017](https://doi.org/10.7554/eLife.01579.017)